Changes in pulmonary function and hepatic flow associated with a surgically induced porto-caval shunt

by

Paul Joseph Antol, Jr.

A Thesis Submitted to the

Graduate Faculty in Partial Fulfillment of the

Requirements for the Degree of

MASTER OF SCIENCE

Major: Biomedical Engineering

Iowa State University
Ames, Iowa

1980

TABLE OF CONTENTS

FOREWORD

The world (parenthetically speaking) has a mistaken notion about the nature of science and scientists . . . scientists often seem to be matter of fact people, unromantic and even hard-headed. That is because the scientific attitude is realistic, as opposed to ritualistic. But there is a vague, continuously satisfying glow of emotion about any science, and he who has accepted and learned its discipline is marked for life. (Markowitz, Archibald, and Downie, 1964, p. 2)

INTRODUCTION

The many effects of alcoholism have been investigated over the years and yet there are many questions that remain to be answered. As it will be described later, chronic alcoholism usually leads to cirrhosis of the liver (or Laennec's cirrhosis), portal hypertension, and other physiological disorders. Such disorders as esophageal varices, ascites, and the establishment of collateral vessels that divert portal blood directly into the systemic circulation are directly correlated with portal hypertension. It is these collateral vessels, either porto-caval or porto-pulmonary shunts, that are of direct interest in this research.

The main purpose of this research is to investigate the effects on pulmonary function of a porto-caval shunt which changes portal flow.

Because of the porto-caval shunt, blood is diverted from the mesenteric and splanchnic vasculature into the vena cava. As a result of this shunt, the lung capillary system receives the metabolites and other absorbed compounds that originate in the gastrointestinal outflow. Therefore, digestive compounds normally removed or altered by the liver may alter pulmonary function.

In the alcoholic human, the study of these effects is complicated by the presence of the liver cirrhosis itself, poor diet, smoking, and the continued abuse of alcohol. Although it has been demonstrated that porto-caval and porto-pulmonary shunts can develop naturally during the progress of the disease, various types of porto-caval anastomoses are performed clinically to relieve the portal hypertensive state.

It has been reported in the literature that humans who have cirrhosis of the liver and a surgical porto-caval anastomosis appear to demonstrate some cardio-pulmonary dysfunction. The cardio-pulmonary dysfunction includes pulmonary hypertension, cardiomegaly, and a hypertrophy of the interstitium of the lung.

Therefore, the question arises as to whether the disorders observed in lung function arise as a result of the cirrhotic liver, the porto-caval shunts, or are due to some other possibility, such as smoking.

In order to demonstrate an altered portal flow and the exposure of the lung to portal blood (i.e., hepatic cirrhosis), porto-caval anastomoses were performed on five healthy dogs. The surgical procedure is known as the Eck fistula (Markowitz et al., 1964, pp. 542-546). Using each dog as its own control, pulmonary and liver function studies were conducted at various times after surgery in an attempt to determine the effects of porto-caval shunts that are independent of the numerous problems created by liver cirrhosis, smoking, and the abuse of alcohol.

REVIEW OF LITERATURE

During the last twenty years, a great quantity of information has been compiled on the effects of alcohol on living organisms. These effects are numerous and occur in many organ systems including heart, liver and the central nervous system, as described by Lieber (1976). More recently, data have been obtained which suggest an interaction of alcohol with the lung. Since alcoholism is such a complex condition with many dysfunctions occurring simultaneously, it remains difficult to ascertain the exact cause or causes for the impairment of lung function (Burch and Depasquale, 1967). This review will attempt to develop a foundation of literature to support the function of porto-caval shunts in the normal and alcoholic individual.

Alcoholism and the Lung

Several studies have looked at pulmonary function in alcoholics. Banner (1973) studied thirty patients described to be long-term, heavy drinkers. Of the eleven patients selected for pulmonary mechanics tests, four had normal pulmonary mechanics, four had signs of airway restriction, one had signs of emphysema, and two were not consistent with any known pulmonary dysfunction. From these data, he suggested that the ultrastructure of the lung may be damaged by alcohol. Emirgil et al. (1974) reported a decrease in total lung capacity, vital capacity, and residual volume in twenty-three chronic alcoholics. They suggested alcohol as a causative agent in producing lung disease independent of the effects of smoking or previous pulmonary infection. Emirgil and Sobol (1977) con-

firmed the results of Banner (1973) and stated that little information exists with regard to the effects of alcohol or the effects of alcohol metabolites on the lungs. Furthermore, Emirgil and Sobol observed impaired lung function could be related to hepatic dysfunction, not to the alcohol itself.

Ruff et al. (1971) reported that in 80% of the hepatic cirrhosis cases studied, the closing volume (the lung volume at which the dependent lung zones begin to trap gas as a result of airway closure) was increased and exceeded the functional residual capacity (FRC). This indicates some of the airways are closed during normal breathing. Two suggestions for premature closure were made: 1) the loss of elastic recoil in the dependent zones of the lungs, and 2) a decrease in resistance during mechanical compression of the small airways from distended vessels and from interstitial pulmonary edema.

It was suggested by Ruff et al. (1971) that the compression of small airways and presence of interstitial pulmonary edema was responsible for the impaired diffusion and lowered arterial oxygen levels in cases of liver cirrhosis. Although no direct evidence of pulmonary edema was found by Ruff et al., separate necropsy studies by Berthelot et al. (1966) and Cameron (1948) not only demonstrate dilatation of precapillary sphincters, but also pulmonary edema in cases of cirrhotic patients.

Heinemann (1960) proposed the lowered arterial oxygen levels were due to venous-to-arterial shunts. He observed that administration of 100% oxygen to patients with liver disease experiencing hypoxemia did not abolish the problem of hypoxemia.

Effects of Portal-Systemic Anastomoses

Cirrhosis of the liver is accompanied by marked changes in the hepatic and splanchnic vasculature. This leads to reduced hepatic blood flow, increased portal venous pressure, and the development of collateral vessels. The formation of collateral vessels allows portal blood to by-pass the diseased liver. The portal blood enters either the inferior vena cava through porto-caval shunts or the superior vena cava through porto-pulmonary shunts (Bradley et al., 1952; Taylor and Myers, 1956; and Heinemann, 1960, 1977).

Calabresi and Abelmann (1957), indicated that lowered arterial oxygen tensions may be due to either uneven ventilation-perfusion relationships or to anatomical shunts bypassing the lungs from the portal vein. They demonstrated anatomical shunts created by anastomoses of the portal bed with the superior vena cava and pulmonary vein. Their data defined the shunts as follows: 1) a porto-caval shunt would exist when blood passes from the portal vein through the peri-esophageal and the mediastinal or azygos veins to the superior vena cava, and 2) a porto-pulmonary shunt would exist when blood passes from the portal vein through the peri-esophageal and mediastinal veins to the bronchial veins and finally to the pulmonary vein. A porto-pulmonary shunt would therefore bypass the lungs and result in the lowering of arterial blood oxygen levels (Calabresi and Abelmann, 1957).

Heinemann (1960) supported the findings of Calabrasi and Abelmann (1957) by suggesting the volume of porto-pulmonary shunted blood depends on the available pressure gradient. Heinemann also suggested that

metabolites from the gastrointestinal tract would have direct access to the pulmonary arteries via cirrhotic shunted or surgically induced anastomoses of the portal vein to the vena cava. He points out that the development of cardiac hypertrophy, particularly predominant right ventricular hypertrophy, occurs in patients with liver cirrhosis. Since cardiac output is elevated in cirrhotic patients, it would account for the occurrence of pulmonary hypertension as well as cardiac hypertrophy. However, Heinemann alludes to the idea that vasoactive substances drained by the splanchnic vessels and normally inactivated by the liver could reach the pulmonary and systemic circulation via the collateral vessels.

Shaldon et al. (1961) concluded there was no relationship between arterial oxygen unsaturation and porto-pulmonary anastomoses, which is contrary to Calabresi and Abelmann (1957) and Heinemann (1960).

The difference in opinion between Shaldon et al. (1961), and Calabresi and Abelmann (1957) and Heinemann (1960) was further complicated by Williams and Abelmann (1963), who measured porto-pulmonary shunt flow in one patient as 27% of total portal flow, and also by Nakamura et al. (1965), who measured shunt flows in two patients at 11% and 14%. However, both Williams and Abelmann and Nakamura et al. agreed on two points:

1) Arterial oxygen unsaturation is not due to the shunts, which supports Shaldon et al. (1961).

2) The shunts may permit substances from the portal venous bed to pass directly into the systemic circulation, thus bypassing the liver and the lungs altogether, which supports Heinemann (1960).

Porto-Caval Shunts and Hepatic Flow

The discrepancy in this review concerning anatomical porto-caval and porto-pulmonary shunts and their effects is complicated by the surgical treatment for portal hypertension in advanced cases of cirrhosis. In cirrhotic patients who are afflicted with either bleeding esophageal varices or the buildup of ascitic fluid due to increased pressure in the portal vasculature, the treatment is to create a porto-caval shunt. This is usually done with either a side-to-side or an end-to-side surgical anastomosis of the portal vein to the vena cava. This results in part or all of the portal blood being diverted directly into the systemic vasculature and the portal system undergoes decompression (Shackelford, 1955, pp. 677-688).

Bradley et al. (1952, 1953) observed hepatic circulation in cirrhosis and saw that hepatic blood flow decreased during any cirrhotic process. They stated that hepatic ischemia and relative tissue hypoxia appear to be characteristic stigmas and speculated that changes in hepato-cellular oxygen metabolism may reflect some serious derangement of cellular physiology. These changes may be followed by necrobiosis and alteration in the tissue and vascular structure of the liver.

Porto-Caval Shunts and Pulmonary Function

Cotes et al. (1968) evaluated lung function on three patients who had porto-caval anastomoses performed five to six years previously. In observing dilatation of the precapillary vessels of the lung, however, they point out that because the surgery decompresses the portal system, there

should be no blood flow through any of the porto-pulmonary shunts which may have been present. Cotes et al. proposed precapillary pulmonary vasodilatation to be one of the consequences of reduced portal blood flow. There was evidence in the three patients for the syndrome of defective gas transfer, which is usually accompanied by features suggestive of fibrosing alveolitis. They concluded that the surgical technique which prolongs the lives of these cirrhotic patients may increase the incidence of further pulmonary complications.

Sallam and Watson (1970) discussed complications arising in the lung as a result of micro-thromboemboli originating in the splenic and portal veins. They described a porto-caval anastomosis performed on a patient diagnosed with Banti's syndrome six years previously. Although pulmonary function tests and biopsy of the liver were shown to be normal, there was considerable evidence of pulmonary hypertension as seen in X-ray films. Sallam and Watson came to no conclusion in this study other than the problem was probably due to a thrombus in the splenoportal system releasing microemboli.

Senior et al. (1968) conducted pulmonary function studies on four patients with hepatic cirrhosis and surgical porto-caval shunts. These patients had clinical signs of pulmonary hypertension with cor pulmonale and normal chests as evidenced by ECG and chest X-rays prior to porto-caval anastomosis. On later examinations, there were marked changes in ECG indicative of right ventricular hypertrophy, and in the radiologic films which showed evidence of cardiac enlargement and dilatation of the main branches of the pulmonary artery. Pulmonary parameters and cardiac

outputs were normal while minute alveolar ventilation and pulmonary arterial pressure were abnormally elevated. Arterial hemoglobin saturation was reduced (hypoxemia). Necropsy studies on two of these patients showed microscopic evidence of thromboemboli in small pulmonary vessels. The evidence included intimal thickening, medial hypertrophy, and partial occlusion and recanalization of vessel lumens. However, no sources of the thromboemboli were found at autopsy.

Lebrec et al. (1979) observed the same symptoms as Senior et al. (1968) in nine patients with similar histories of hepatic cirrhosis and surgical porto-caval anastomosis. They concluded that diversion of portal venous blood into the inferior or superior vena cava plays a major role in the development of pulmonary hypertension. Lebrec et al. suggested a vasoconstrictive agent produced in the splanchnic territory could bypass the liver and gain access to the pulmonary arteries, thus inducing pulmonary hypertension.

Johnson and Lambert (1967) studied changes in cardiac output in normal dogs that were given end-to-side porto-caval anastomosis. Mortality rate was 50% due to factors outside of the surgery and its consequences. Of the survivors, mean cardiac output was shown to increase 35%. They proposed that the increase in cardiac output was the result of a cyclic pattern in which portal blood flows into a low resistance system (i.e., the inferior vena cava) through the shunt. This results in an increased arterial inflow to the portal system, increasing total portal flow which increases venous return. Increased venous return results in a greater stroke volume and hence, an increased cardiac output. However,

Johnson and Lambert observed a decrease in blood pressure and no change in pulse rate or right atrial pressure.

In summary, this literature review has suggested that alcoholism and the resulting cirrhosis causes numerous complications in lung, heart and liver. Pulmonary hypertension, increased cardiac output, and decreased hepatic blood flow are the major effects of cirrhosis of the liver. However, it remains difficult to separate the effects of cirrhosis and alcoholism from the effects of the clinical treatment for the resultant portal hypertension: the porto-caval shunt.

MATERIALS AND METHODS

Surgical Preparation

Six normal, healthy adult mongrel dogs ranging in weight from 13.6-22.7 kg were obtained and housed at Laboratory Animal Resources, Iowa State University. Porto-caval anastomoses were created surgically using the technique for the straight Eck fistula previously described by Markowitz, Archibald, and Downie (1964, pp. 542-546). The procedure for the Eck fistula is detailed in Appendix A. This surgery created a 1-2 cm fistula between the portal vein and the vena cava just above the splenic vein in each dog. This allowed portal blood to bypass the liver and gain access to the lung vasculature.

No major problems were associated with each approximately six hour surgery and each dog was up and walking twelve to eighteen hours after surgery. Only one dog, #1656, experienced a post-operative localized skin infection from suture. Antibiotic treatment effectively controlled the infection.

Dog #1582 was used only to test the surgical procedure and was not subjected to pulmonary function testing but was included in histopathological examinations at termination.

Pulmonary Function Tests

Dogs #1588, 1598, 1656, 1704, and 1740 were treated similarly in all pulmonary measurements. While under Surital^{R} (Parke-Davis and Company, Detroit, Michigan) anesthesia (22 mg/kg), the animals were intubated and

placed in dorsal recumbency. A 50 cm 7-French catheter imbedded into a rubber stomach tube was filled with normal saline and was then inserted into the esophagous to about mid-thorax. The animal was then connected via the endotracheal tube to a Fleisch^{R} #0 pneumotach (Instrumentation Associates, Inc., New York, New York) which was attached to a Statham^{R} PM5 differential pressure transducer (Statham Laboratories, Inc., Hato Rey, Puerto Rico) for measurement of airflow. Volumes were determined by electronic integration and all measurements of flow, volume, and esophageal pressure were measured on a four-channel Beckman^{R} R611 Dynagraph (Beckman Instruments, Inc., Schiller Park, Illinois). All channels were balanced and calibrated before measurements. The esophageal cannula was connected to a Statham PR23 low-pressure transducer and after flushing with normal saline, the position of the esophageal cannula was adjusted to give a slight positive peak at the onset of expiration. After the animal and physiological recordings were stable, a continuous recording (25 mm/sec) for one minute was obtained. Compliance (C) and resistance (R) values were then determined.

Functional residual capacity (FRC) measurements were conducted using a multiple breath nitrogen washout method. The dogs were attached to a digital nitrogen analyzer (Hewlett-Packard^{R} #47302A, Hewlett-Packard, Inc., Palo Alto, California) and a digital pneumotach (Hewlett-Packard^{R} #47303A). Values for nitrogen content and inspired tidal volume were taken from the analog outputs of both devices and recorded on a two-channel Brush^{R} 220 recorder (Gould, Inc., Cleveland, Ohio). When the pattern of respirations appeared stable, the animal was changed from

breathing room air to 100% oxygen. At the same time, expired air was collected in an evacuated meterological balloon. When the expired nitrogen content fell below 10% in each breath, the animal was removed from the pneumotach and the nitrogen content of the expired air in the balloon was determined with the nitrogen analyzer. Two separate FRC measurements were performed and the results were averaged.

Samples for blood gas determination were drawn when the nitrogen content returned to normal, allowing the blood to re-equilibrate after FRC measurement. Blood gases were measured on an Instrumentation Laboratories^{R} 513 blood gas analyzer (Instrumentation Laboratories, Lexington, Maryland) and values for pH, partial pressure of carbon dioxide (PCO_2), and partial pressure of oxygen (PO_2) were obtained. The arterial blood was sampled from either the right or left femoral artery and the venous blood was sampled from either the right or left cephalic vein.

Liver Function Tests

The function of the liver was determined by injection of a calculated amount of sterile indocyanine green (Cardio Green^{R}, Hynson, Westcott, and Dunning, Baltimore, Maryland) and observing the clearance of the dye from the blood over a time period of twenty minutes.

Each animal was restrained, but not anesthetized, and a 20-gauge 3.8 cm intravenous catheter (IV) was introduced into the cephalic vein. After withdrawing a 10 ml zero-time sample, an amount of the dye equivalent to 0.5 mg/kg was injected through a 20-gauge needle into the opposite cephalic vein. A timer was started immediately upon injection of the dye

and blood samples were withdrawn through the intravenous (IV) catheter at times of 1, 5, 10, 15, and 20 minutes post-injection. Blood samples were then added immediately to test tubes containing 0.1 ml of 1% (1 g/100 ml saline) heparin, and were centrifuged at maximum speed in a clinical centrifuge for ten minutes. After the plasma was removed from the packed cells, the amount of indocyanine green in the plasma was determined spectrophotometrically at 805 nm and calculated from a standard curve. If the absorbance was greater than 0.8, dilutions were made to increase the accuracy of the determination. In most cases, no more than a 1:3 dilution was required. The clearance curves for the dye were then produced by plotting on a semi-logarithmic scale concentration (mg/100 ml) vs. time for each dog. The clearance curves were subjected to a linear regression program and a correlation coefficient was determined to verify the linearity of the clearance relationship. Five experimental and two normal dogs were tested on two separate occasions.

Clinical Tests

Blood samples were drawn four days prior to euthanasia and analyzed by the Clinical Laboratory, Department of Veterinary Pathology, Iowa State University. The levels of blood urea nitrogen (BUN), glucose, bilirubin, albumin, alanine amino transferase (≅SGPT), and alkaline phosphatase were assayed with the assistance of Dr. A. E. Ledet, Department of Veterinary Pathology, Iowa State University. The clinical tests listed were selected in order to obtain information which might indicate liver abnormality.

A measurement of activated clotting time (ACT) was also made using Vaccu-Tainer^{R} #3865 tubes (Becton-Dickinson and Company, Rutherford, New Jersey). Elevated clotting time would give an indication of abnormal liver function at the cellular level since the majority of the clotting proteins are synthesized by the liver (White et al., 1973, Chapter 30).

Post-Mortem

Animals were euthanized at an average of 32 weeks from the time of pre-surgical measurements. Samples of brain, lung, heart, liver, jejeunum, kidney, spleen, thyroid, and parathyroid were sectioned and examined by Dr. Robert Glock, Department of Veterinary Pathology, and Dr. John Andrews, Diagnostic Laboratory, College of Veterinary Medicine, Iowa State University. The portal vein and vena cava in the vicinity of the shunt were ligated and removed in order to establish the amount of patency in the shunt.

CALCULATIONS

Lung Compliance, Resistance, and Functional Residual Capacity

Lung compliance and resistance are calculated from values for airflow, tidal volume, and esophageal pressure (Figure 1). A perpendicular line is drawn through the recordings at zero airflow and at maximum airflow. When the airflow is zero, there is no effort required by the lung to overcome airway resistance and, therefore, the tidal volume and esophageal pressure are due only to the elastic resistance of the lung at that point. Consequently, compliance can then be calculated using the tidal volume (V_T) and the esophageal pressure (P_T) at zero airflow:

$$\text{Compliance } (C_L) = V_T/P_T \qquad (\text{L/cm } H_2O)$$

From the perpendicular line drawn at maximum airflow, a tidal volume at a flow (V_{TF}), a pressure at a flow (P_{TF}) and the value for the flow (F) are determined. Assuming lung compliance is constant over the range of tidal volumes, the esophageal pressure required to overcome elastic resistance (compliance pressure) at a given lung volume may be calculated:

$$\text{Compliance pressure } (P_{C_L}) = V_{TF}/C_L \qquad (\text{cm } H_2O)$$

This pressure is subtracted from the total esophageal pressure measured at an airflow to yield the pressure generated to overcome airway resistance to airflow:

$$\text{Resistance pressure } (P_R) = P_F - P_{C_L} \qquad (\text{cm } H_2O)$$

The resistance of the airways to airflow is calculated from the resistance pressure and the measured flow (F):

$$\text{Resistance } (R) = P_R/F \qquad (\text{cm } H_2O/\text{L/sec})$$

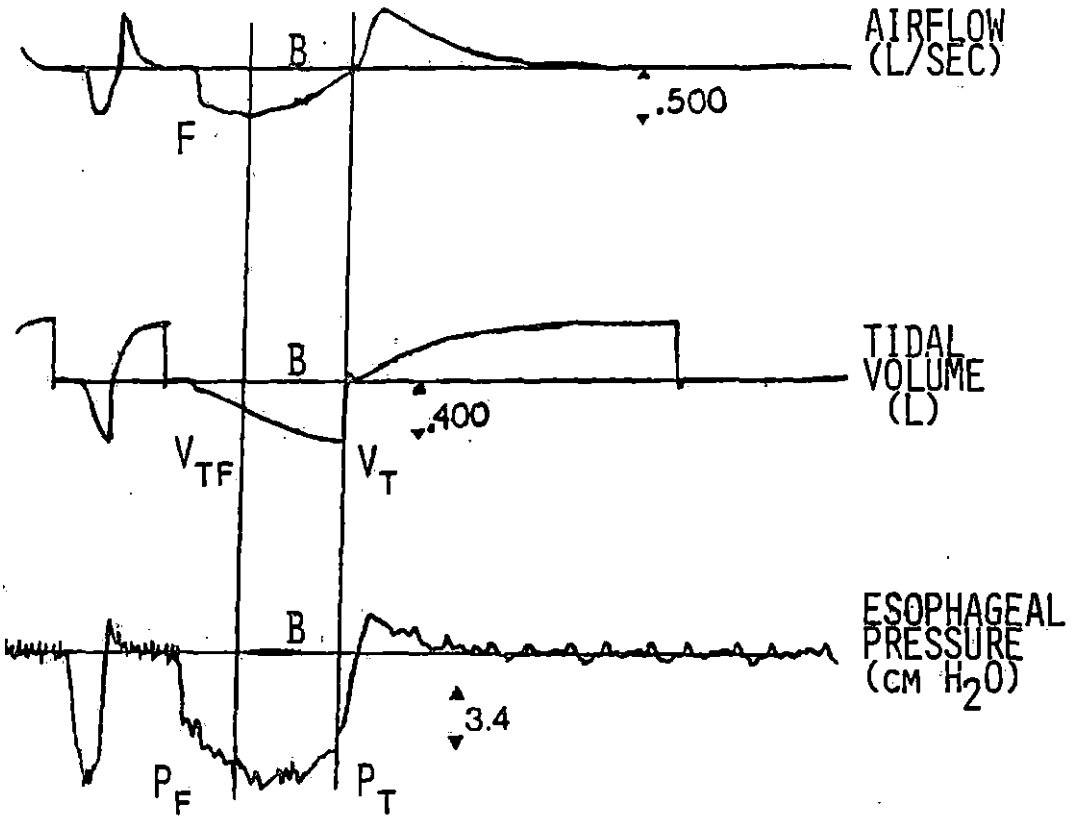

Figure 1. Recording used to calculate lung compliance (C_L) and airway resistance (R) (Engwall, 1980)

F = maximum airflow
V_T = maximum tidal volume
V_{TF} = tidal volume at maximum airflow
P_T = esophageal pressure at maximum tidal volume
P_F = esophageal pressure at maximum airflow
B = baseline

FRC was calculated from the following formula (Figure 2):

$$FRC = (V_E + V_{DS}) \times (F_E - F_I)/(F_O - F_A) \quad \text{(ml)}$$

where V_E = volume of expired air during washout (ml)

V_{DS} = dead space of the apparatus (about 45 ml)

F_E = content of nitrogen in the expired air

F_I = content of nitrogen in the inspired oxygen

F_O = content of nitrogen in the alveoli pre-washout

F_A = content of nitrogen in the alveoli post-washout

Since lung compliance and resistance can be affected by the frequency of respiration, all values have been normalized by dividing by the frequency. Since FRC is affected by body weight, those values were corrected by dividing by the individual weights.

Liver Function

From the clearance curves for indocyanine green, the percentage disappearance rate was calculated using the following formula:

$$\text{Percentage Disappearance Rate (PDR)} = (1 - e^{D}) \times 100$$

$$D = (\text{Ln } C_2 - \text{Ln } C_1)/(T_2 - T_1)$$

where C_1 = concentration at time T_1 (mg/100 ml)

C_2 = concentration at time T_2 (mg/100 ml)

All calculations were performed on a programmable TI-55^R calculator (Texas Instruments, Incorporated, Dallas, Texas). Programs for the calculation of C, R, FRC, and PDR are detailed in Appendix B.

Figure 2. Recording used for calculation of functional residual capacity (FRC) (Engwall, 1980)

A. Nitrogen content
   F_A = content of nitrogen in the alveoli at the end of the washout
   F_E = content of nitrogen in collected expired air
   F_I = content of nitrogen in inspired oxygen
   F_0 = content of nitrogen in the alveoli at the onset of of the washout
   Z = zero line

B. Expired volume
   V_E = total volume of air expired during the washout
   Z = zero line

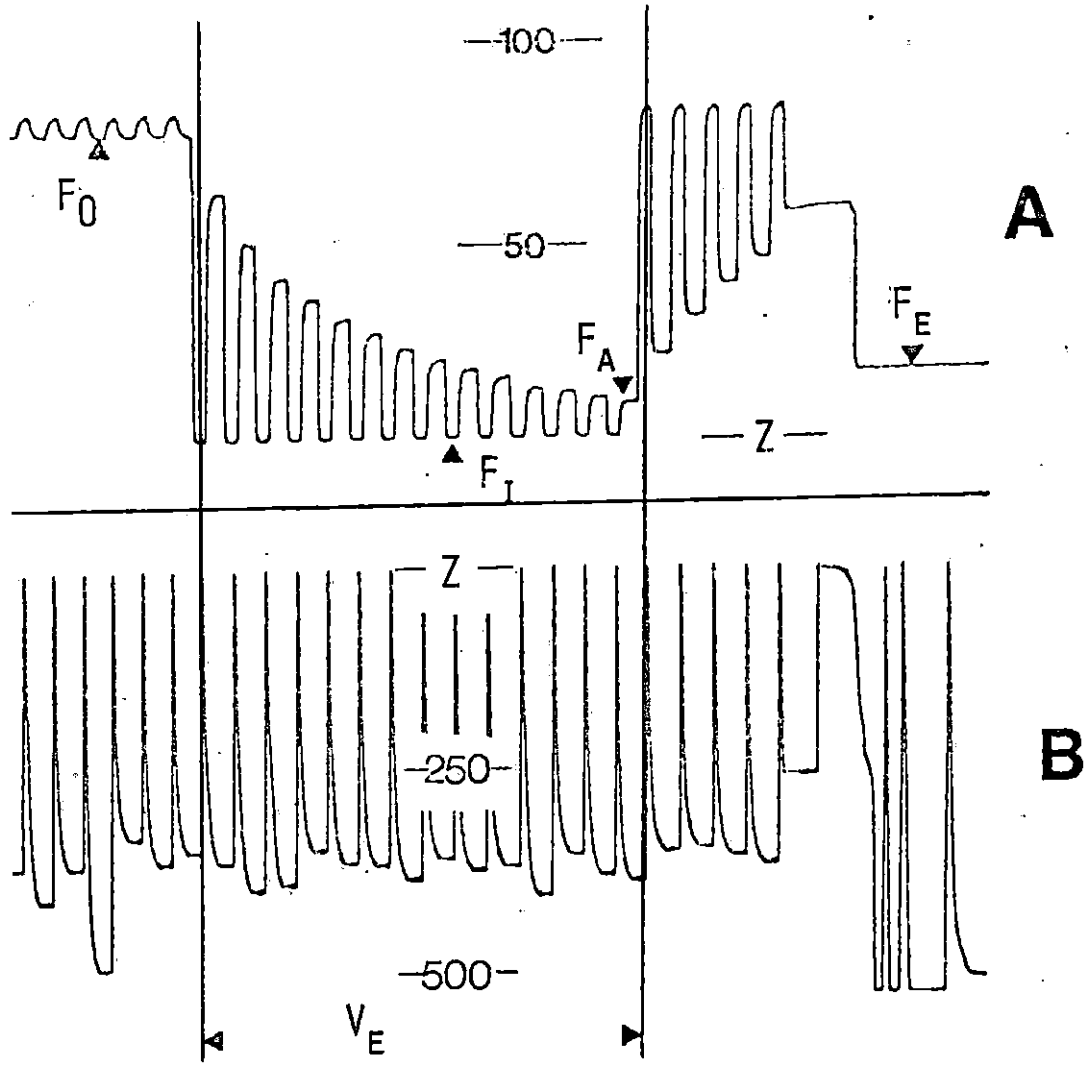
100
50
F0
FA
FE
FI
Z
A
Z
250
500
VE
B

Statistical data were provided by the SAS computer system, Iowa State University, with the assistance of D. J. Meerdink, Department of Nutritional Physiology, Iowa State University.

RESULTS

Pulmonary Function

Results of the pulmonary function tests performed on the five dogs are listed in Table 1. Measurements of compliance (C), resistance (R), and functional residual capacity (FRC) were performed on all dogs at selected times during the experimental period.

Control values are designated in period 1 for all measurements. They are within the limits determined in our laboratory for normal dogs and are also within the range reported by Engwall (1980).

Four of the five dogs studied showed 66.6% decreases in compliance in the first 10-12 weeks after surgery. Three of those four then returned to control in subsequent weeks. The fifth dog showed a 26.5% increase in compliance which then decreased to approach the control value by the 18th week.

Three of the five dogs exhibited a 46.3% increase in resistance during the first 10-12 weeks but subsequently returned to control levels. The other two dogs showed 42.5% decreases in resistance in the first eight weeks, followed by sharp increases averaging 100% in the next two weeks, and then subsequent return toward normal by the 18th week.

Functional residual capacity (FRC) increased 16.3% in four dogs and decreased 25.8% in one dog during the initial 10-12 weeks. However, no dog returned to normal values and FRC remained either elevated or depressed at termination.

Table 1. Pulmonary function data

Period[a]	Dog #	Compliance/f[b]	$\bar{X}$ + S.E.M.	Resistance/f[c]	$\bar{X}$± S.E.M.	FRC/B.W.[d]	$\bar{X}$± S.E.M.	Mean PO_2[e]	Mean PCO_2[e]	mean pH[e]
I	1588	0.0049		1.15		45.0				
(0)	1598	0.0119		0.38		51.2				
	1656	0.0079	0.0117	0.41	0.91	59.0	50.2	85.9	48.1	7.342
	1704	0.0160	±0.0024	1.66	±0.24	53.9	±3.0	±21.4	±2.9	±0.044
	1740	0.0179		0.96		42.1				
II	1588	0.0131		0.97		40.6				
(7.8)	1598	0.0068	0.0080	0.19	0.81	47.8	54.4			
	1656	0.0039	±0.0019	0.84	±0.22	65.7	±5.3	104.9	41.5	7.394
	1704	0.0343		1.08		67.8		±8.5	±13.4	±0.091
	1740	0.0083		1.22		50.3				
III	1588	0.0062		1.41		33.4				
(9.8)	1598	0.0041	0.0047	1.05	1.31	58.6	54.3			
	1656	0.0032	±0.0006	1.39	±0.23	62.9	±5.5	99.1	46.0	7.361
	1704	0.0060		2.05		63.3		±7.5	±6.2	0.019
	1740	0.0038		0.65		53.4				

[a] Mean time (weeks) after surgery.

[b] L/cm·H_2O/bpm.

[c] cm H_2O/L/sec/bpm.

[d] ml/kg.

[e] ±1 S.D.

Table 1. (Continued)

Period	Dog #	Compli-ance/f	$\bar{X}$±S.E.M.	Resist-ance/f	$\bar{X}$± S.E.M.	FRC/ B.W.	$\bar{X}$± S.E.M.	Mean PO_2	Mean PCO_2	mean pH
IV	1588	0.0051		0.36		31.8				
(17.8)	1598	0.0104	0.0098	0.36	0.83	46.0	57.2			
	1656	0.0029	±0.0026	0.39	±0.28	64.0	±8.5	91.6[f]	43.2[f]	7.410[f]
	1704	0.0163		1.54		81.3		±12.7	±5.4	±0.016
	1740	0.0145		1.51		62.9				
V	1588	0.0050		1.09		28.2				
(31.8)	1598	0.0106	0.0096	0.35	0.93	75.5	60.1			
	1656	0.0031	±0.0026	0.60	±0.21	51.9	±9.6	90.5	41.6	7.370
	1704	0.0176		1.56		82.8		±8.3	±3.4	±0.048
	1740	0.0118		1.04		62.1				

[f] $n = 4$.

Since the surgical procedure on all five dogs was not performed on the same day, the time of pulmonary function measurements after surgery was variable for each dog. Therefore, the times of measurement from the initial were averaged along with the individual measurements of C, R, and FRC to aid in the statistical evaluation. By averaging these data, the time after surgery was condensed into five periods and the means and standard error were calculated.

There was a significant decrease ($P < 0.05$) in compliance (Figure 3) from the control for all five dogs. This was accompanied by a concurrent significant increase ($P < 0.05$) in resistance (Figure 4). The mean FRC showed an increasing trend overall, but the increase was not significant (Figure 5).

The changes in mean arterial oxygen content (PO_2), carbon dioxide (PCO_2), and pH were not significantly different from the control.

Liver Function Tests

The results from the liver function tests including percentage disappearance rate and correlation coefficients from the clearance curves are given in Table 2. The data for analysis 1 were obtained at an average of 19 weeks after surgery for all animals. The percentage disappearance rate for each animal during both liver function analyses shows no significant difference between the first and second analysis, which was made seven weeks later at an average of 26 weeks after surgery.

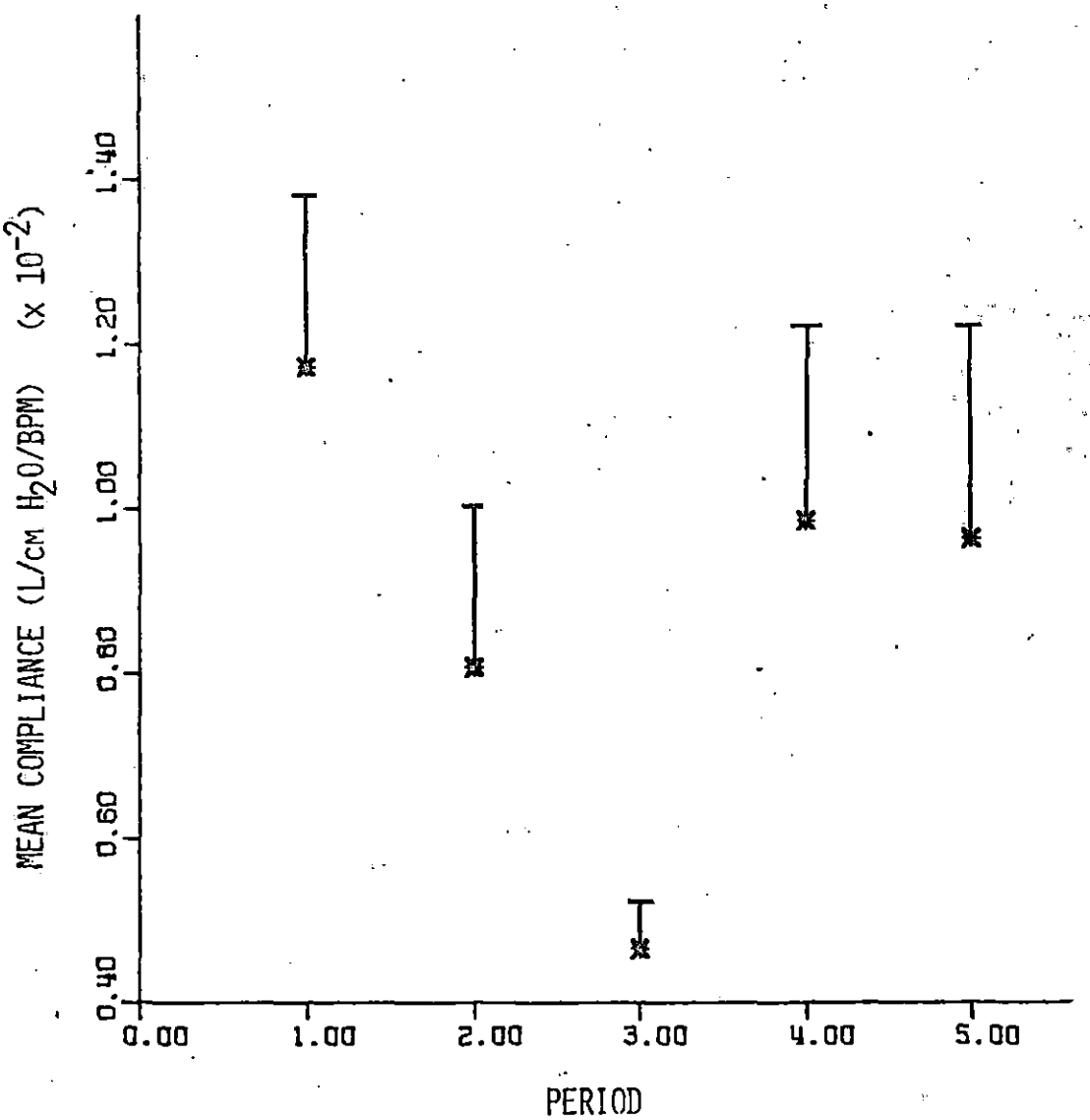

Figure 3. Mean compliance vs. mean time post-op; compliance values are averages for five dogs and are plotted against time periods; the change between period 1 (control) and period 3 is significant ($P < 0.05$)

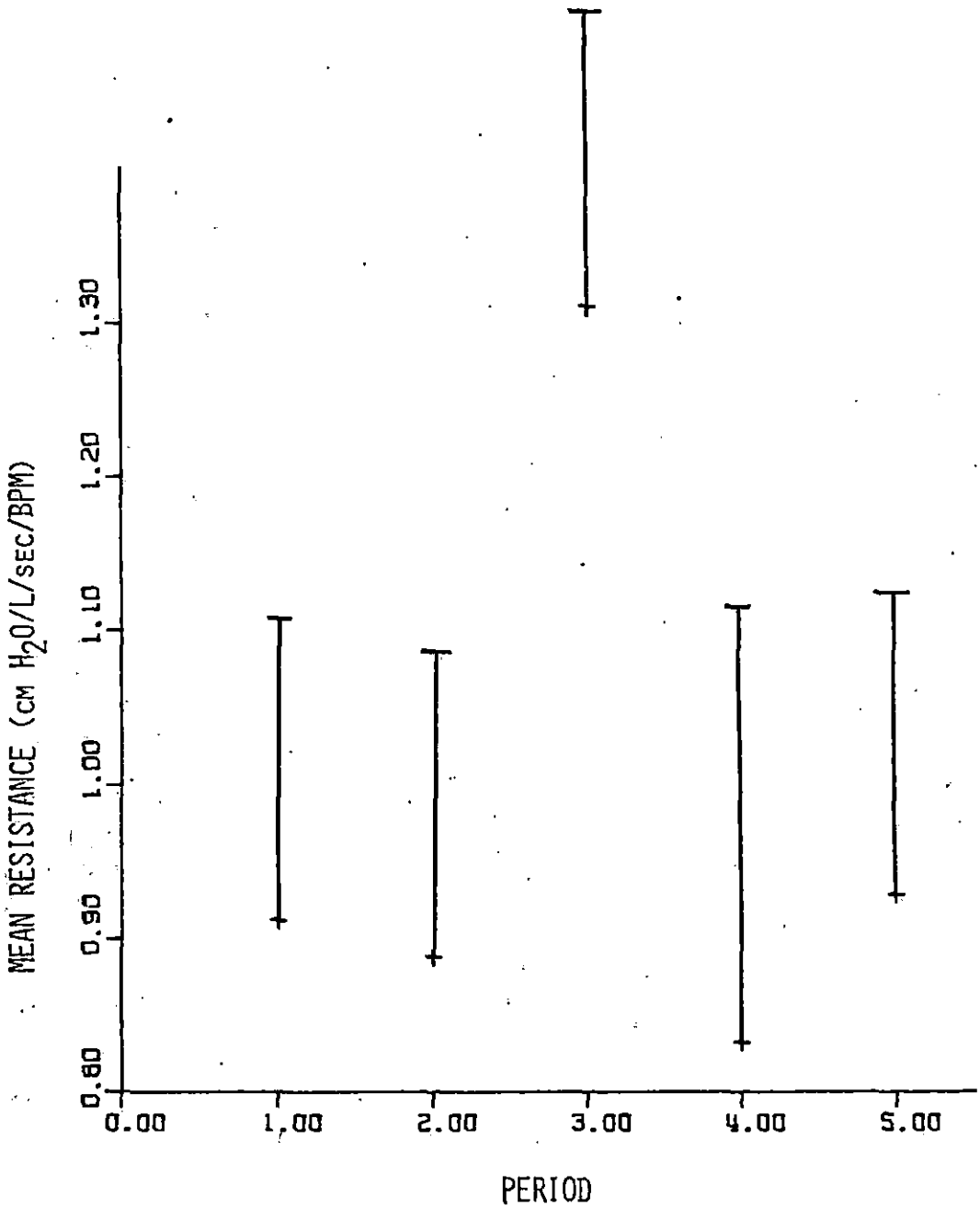

Figure 4. Mean resistance vs. mean time post-op; resistance values are averages for five dogs and are plotted against time periods; the change between period 1 (control) and period 3 is significant ($P < 0.05$)

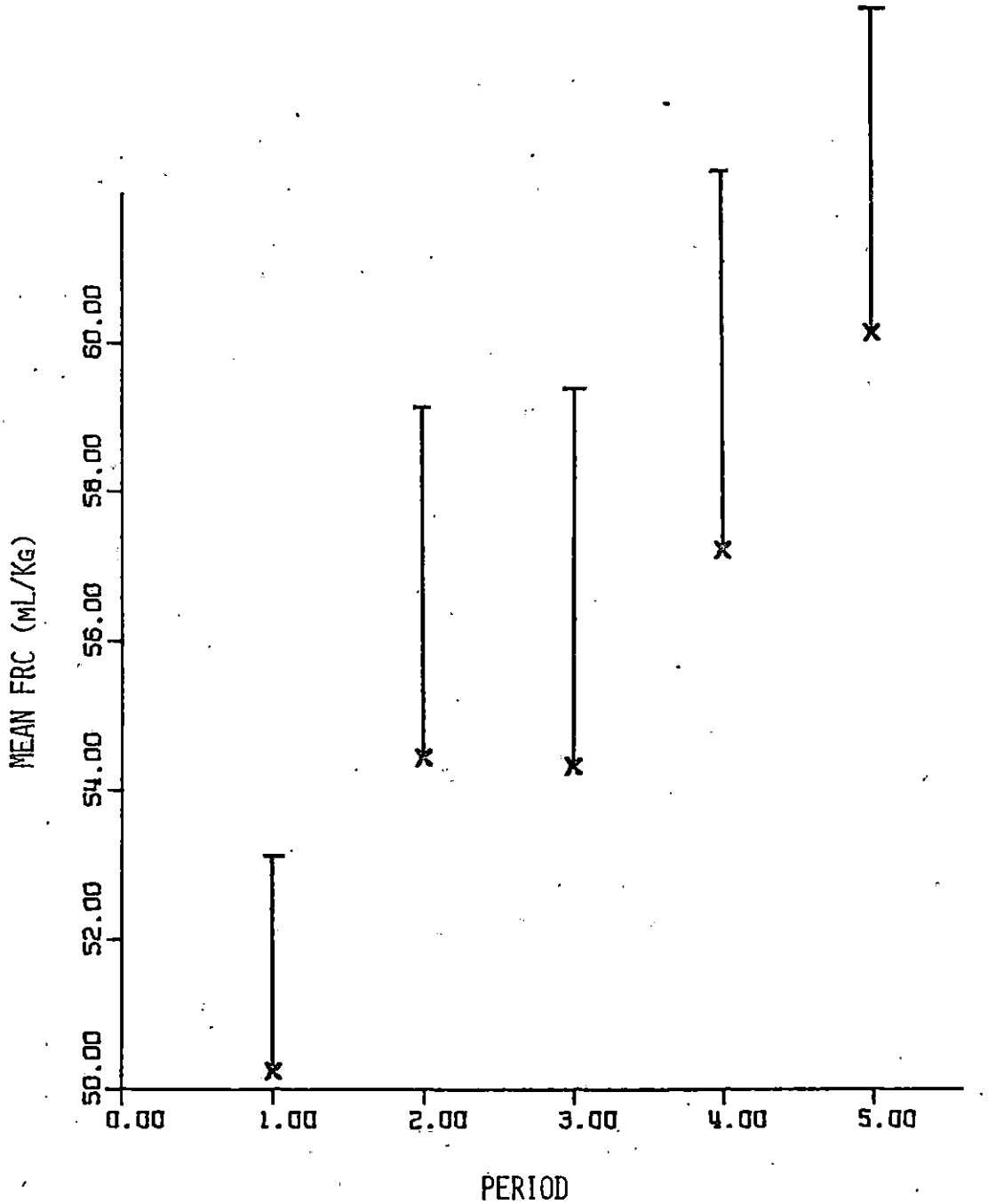

Figure 5. Mean functional residual capacity (FRC) vs. mean time post-op; FRC values are averages for five dogs and are plotted against time periods

Table 2. Results of liver function analysis - percentage disappearance rate (PDR)

	Analysis 1[a]		Analysis 2[b]		
Dog #	PDR	Corr. coeff.	PDR	Corr. Coeff.	Remarks
1588	6.1	-1.000[c]	9.7	-1.000	Shunted
1598	8.6	-1.000	9.2	-0.983	Shunted
1656	10.5	-1.000	12.5	-0.965	Shunted
1704	8.2	-0.945	4.1	-0.994	Shunted
1740	10.6	-0.993	8.2	-0.982	Shunted
1712	-		8.6	-0.993	Normal
1778	-		13.4	-0.961	Normal

[a]Performed at an average 19 weeks post-op.

[b]Performed at an average 26 weeks post-op.

[c]-1 = perfect correlation.

Clinical Tests

The results of the clinical blood analyses including the activated coagulation times (ACT) for all five dogs are displayed in Appendix C. All values were normal at termination.

Post-Mortem Observations

Post-mortem examination results for all six surgical animals indicate that all animals demonstrated mild to moderate right heart dilatation. Two of the dogs showed mild congestion in the lung, and four dogs showed congestion in the liver (Appendix D). Although three dogs showed signs of hookworm infestation, all other structures appeared normal in each dog.

Gross examination of the portal vein and vena cava in the vicinity of the shunt revealed a nonpatent shunt in all dogs. Judging by the condition of the vessels, the shunt had been closed for some time.

Histopathological examination revealed all animals to have varying degrees of fibrosis and congestion in the liver, and also varying degrees of interstitial thickening, fibrosis, and congestion in the lungs. Most other sections showed no major lesions.

DISCUSSION

The Fate of the Shunt

At termination of the experiment that the shunts were closed and apparently had been nonfunctional for some time. This finding immediately ruled out the major assumption made at the beginning of this project. The assumption the shunts would remain patent indefinitely was based on two reasons: 1) the pressure gradient between the portal vein and the vena cava would increase blood flow through shunt; and 2) since the vena cava is a lower resistance system than the liver, there would be a tendency for blood flow to pass through shunt. From these experimental data, the two reasons appear valid for only the first ten weeks after surgery.

In preliminary research by the author, the portal pressure at the level of the splenic vein in one normal dog was 8 mmHg. Taylor and Myers (1956) found portal pressures in normal cats to range from 5-13 mmHg with a mean pressure of 8 mmHg. The pressure in the vena cava at the level of the liver is 2 mmHg (Swenson, 1977, p. 135). Therefore, the pressure difference between the two vessels could be predicted to be 6 mmHg.

If the portal vein had been ligated as outlined in the original procedure (Markowitz et al., 1964), there is no doubt patency would have been maintained. However, the complications from a complete shunt may have been a greater problem. Markowitz et al. described in detail the symptoms of meat intoxication in dogs with complete Eck fistulas. They noted recurring instances of coma and lethargy in shunted dogs. Johnson and Lambert (1967) reported similar problems in their dogs. They reported

losing 50% of their animals due to the same complications described by Markowitz et al.

Because the portal vein was not ligated, the problems reported by Markowitz et al. (1964) and Johnson and Lambert (1967) were not experienced in this project. The liver was able to receive some portal blood.

The apparent reason for shunt failure can be attributed to not ligating the portal vein and possibly the method for producing the shunt. The cut edges of the vessel walls would have provided enough connective tissue surface that platelets and fibrin strands could have been laid down immediately following surgery. Since the predicted pressure difference was small, it remains doubtful the shunt flow would have been enough to prevent further deposition of material in the shunt. Therefore, the shunt would gradually become sealed over time.

Pulmonary Studies

Although the fistula failed, there was still a marked change observed in both pulmonary structure and function. In all dogs subjected to pulmonary studies, the maximum change in compliance and resistance values occurred at an average of ten weeks after surgery (period 3). After ten weeks post-surgery, compliance and resistance values approached pre-surgery levels. Although a positive correlation cannot be made, the return of pulmonary measurements to normal may indicate the closure of the shunt. Functional residual capacity (FRC) increased slightly. These changes can be explained by the microscopic structural changes in the

lung. There were marked signs of interstitial thickening and pulmonary edema accompanied by varying degrees of fibrosis in the dog lungs.

In cases of pulmonary edema, compliance decreases due to reduction in lung volume and interference with the elastic properties in the lung. Concurrently, lung resistance increases due to the narrowing of the small airways as a result of the thickening of the peribronchial cuff. FRC usually increases when there is an increase in airway resistance. The presence of fibrotic areas would also tend to decrease compliance, but resistance and FRC would tend to either remain normal or decrease slightly (West, 1977).

The changes observed in compliance, resistance, and FRC may be due to not only interstitial edema but also to the presence of microemboli, which were most prominant in dog #1582. Microemboli could play a part in the development of pulmonary hypertension (Sallam and Watson, 1970). There was considerable right heart dilatation observed in all dogs which may have been produced by pulmonary hypertension. The various factors that lead to pulmonary hypertension include obliteration of the capillary bed by destruction of alveolar walls or interstitial fibrosis, and hypertrophy of smooth muscle in the walls of small arteries (West, 1977). All dogs demonstrated areas of tissue degeneration and fibrosis in the lung. Dr. Andrews of the Diagnostic Laboratory, Iowa State University, observed that the severity of tissue abnormality in the dogs of this project was correlated to the amount of time passed since surgery was performed.

The literature reported the same findings as this research, only under much different circumstances. The four patient studies by Senior

et al. (1968) demonstrated marked changes in anatomical structure of heart and lungs after surgery for porto-caval anastomosis. Prior to surgery, these patients had liver cirrhosis and portal hypertension. However, after surgery, pulmonary hypertension and cor pulmonale was noted.

In patients with liver cirrhosis, Lebrec et al. (1979) agreed with Senior et al. (1968) that the existence of pulmonary emboli was the cause of the pulmonary hypertension. However, neither Lebrec et al. or Senior et al. could find the source of the emboli at autopsy.

Since no gross thrombi were found in this project, the pulmonary and cardiac abnormalities that were observed are more related to the porto-caval anastomosis than to the liver damage. Unlike the studies by Lebrec et al. (1979) and Senior et al. (1968), all dogs used in this project were normal, healthy dogs. There were no symptoms or direct evidence of liver cirrhosis, portal hypertension, excessive alcohol intake, smoking, or other problems that were experienced by Lebrec et al. or Senior et al. The gross and microscopic abnormalities produced by the shunt in the dogs in this project were still apparent at termination 22 weeks later.

Because the shunt may be responsible for the changes in pulmonary function instead of the liver, the following question arises, "What compound is contained in portal blood that would produce these changes?" In normal systemic circulation, compounds that would be normally detoxified by the liver could cause either the destruction of lung tissue or the formation of microemboli. Both Lebrec et al. (1979) and Heinemann (1960, 1977) have proposed the existence of agents from the splanchnic or mesenteric vasculature passing through the shunt into the general circulation.

There are several possibilities for the nature of this agent:

1) Microemboli that would form normally in the walls of the intestine could reach the lung parenchyma directly through the shunt.
2) Bacterial cells (particularly anaerobes) that gain access to the portal vein from the intestine could exhibit a thrombogenic or vasoconstrictive response when trapped by the lung capillaries. The cell-mediated immune system could cause an edematous response in removing these bacterial cells.
3) Endotoxins from these bacterial cells could exhibit a hypertensive response.
4) The circulating levels of digestion products would become abnormally elevated in the lung capillaries. Particularly, the concentrations of amino acids and fatty acids after a meal would require an increased time to be cleared from the general circulation. This may be enough to cause trauma to the lung vasculature.

Any of the four possibilities mentioned could be responsible for causing the pulmonary hypertension. These suggestions remove the major emphasis from the liver as being the causitive agent responsible for changes in the lung.

Liver Function Studies

All the values for percentage disappearance rate (PDR) are within the range for normal dogs reported by Wheeler et al. (1958). These PDR values are also in agreement with values calculated from data reported by Stekiel et al. (1960). Tests were within the range established by the clinical

laboratory, Iowa State University. It should be noted that in some of the measurements, the values are approaching the limits of normality. The activated coagulation time (ACT) results were within the normal range reported by Byars et al. (1976).

The function of the liver as determined by dye clearance methods allowed the cellular function of the liver to be measured. It would also have allowed information relating to the patency of the shunt to be obtained. However, the dye clearance determinations were performed after the shunt had probably closed. Stekiel et al. (1960) and Banaszak et al. (1960) reported a method to calculate mean hepatic transit time using indocyanine green in dogs. The method required hepatic cannulation with the assistance of a fluoroscope and only total hepatic flow, not portal flow, could be established. Therefore, no simple noninvasive technique is available to measure portal flow or shunt flow without performing laparotomy.

Although liver function was normal at termination, the liver was apparently affected by the presence of the shunt. Histological examination revealed a marked disorganization in the liver parenchyma and an overall fibrosis of the central veins in all dogs. Bradley et al. (1952, 1953) observed similar changes in cirrhotic livers in humans. Hepatic ischemia and tissue hypoxia are common in the cirrhotic process, and these factors were observed in this research. The cellular abnormalities observed in the dogs in this project suggests serious results when portal blood flow is reduced. The liver of the dog is highly dependent on portal blood for oxygen (Swenson, 1977, p. 135).

The values reported for the clinical tests were within the range

established by the clinical laboratory, Iowa State University. It should be noted that in some of the measurements, the values are approaching the limits of normality. The activated coagulation time (ACT) results were within the normal range reported by Byars et al. (1976).

Mathematical Model

A mathematical model of the liver and the shunt was developed to characterize the flow patterns around the liver. The liver was treated as a single pool with two inputs and one output. Output from the lymphatic vessels of the liver is very small and was omitted. Two first-order differential equations were determined for both cases (normal and shunted) and their derivations are given in Appendix E. The resulting equations were programmed on a PDP-8A computer (Digital Equipment Corporation, Maynard, Massachusetts) and the results were displayed on a storage oscilloscope. Figure 6 demonstrates both the normal and shunted hepatic clearance of a liver-specific dye (e.g., indocyanine green). As the shunt diverts increasing amounts of blood away from the portal vein, the ability of the liver to remove the dye from the general circulation becomes lessened and the clearance time increases. When the ratio of normal half-time ($T_{\frac{1}{2}}$) to shunted half-time ($T'_{\frac{1}{2}}$) was calculated, a relationship was established relating this ratio to the product of the shunt fraction (σ) and the ratio of total hepatic venous flow (Q_L) to the hepatic arterial flow (Q_H):

$$\frac{T_{\frac{1}{2}}}{T'_{\frac{1}{2}}} = \sigma \frac{Q_L}{Q_H}$$

From this relationship, the shunt fraction may be calculated if the half-time ratio and the liver flow ratio is known. Therefore, a noninvasive technique may be available to determine the amount of shunt in an animal.

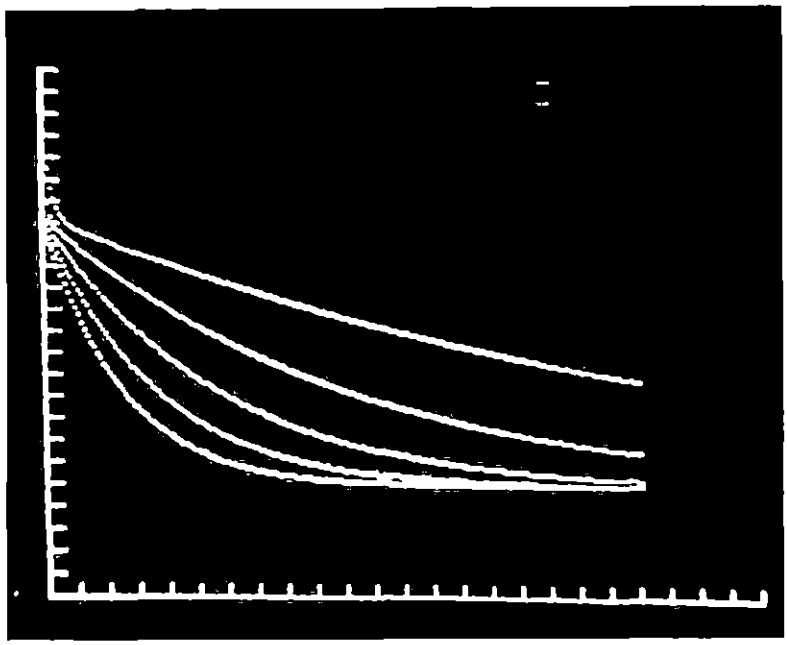

Figure 6. Computer simulated clearance of indocyanine green; the photograph was constructed by the PDP-8A computer using the developed equations. The Y-axis represents concentration and the X-axis represents time. The graph shows predicted change in clearance of the dye. The bottom curve represents 0% shunt while the curves above represent 25, 50, 75, and 100% shunt respectively.

CONCLUSIONS AND RECOMMENDATIONS

In reviewing this research project, there is no doubt regarding the importance of maintaining a patent shunt. The results (or lack of results) obtained depended on a patent shunt at termination. More knowledge concerning the function of the shunt has been obtained and future experiments will be based on this knowledge.

An incomplete shunt (portal vein intact) appears to be patent for only ten weeks. Therefore, a more concentrated study must be devoted to the early period of patency.

A complete shunt (portal vein ligated) or implanted static shunts may be necessary to maintain the patency of the shunt and produce the maximum change in pulmonary and liver function. However, the complications associated with portal ligation would cause adverse conditions that would affect collection of reliable data. Furthermore, there are no cases reported of a complete anatomical shunt. Therefore, the complete shunt would not be an accurate model for the cirrhotic condition.

More data must be collected if changes in pulmonary and liver function are to be more accurately described. This will require more animals and more frequent pulmonary and liver function, and clinical tests. This will hopefully eliminate any possible questions regarding events occurring between long periods of time, which was a problem in this research.

Finally, the mathematical model must be expanded and confirmed by animal experimentation. With the aid of this model, a noninvasive method to determine the shunt fraction from dye clearance data can be improved

and tested. The model would enable the researcher to obtain information regarding the dynamics of a porto-caval shunt without resorting to surgical laparotomy.

SUMMARY

Five normal dogs were given porto-caval shunts using a modified technique of the Eck fistula. Measurements of pulmonary function including compliance, resistance, and functional residual capacity, and arterial oxygen levels demonstrated significant decreases in compliance and increases in resistance. Functional residual capacity and arterial oxygen levels did not change significantly. Liver function determined by clearance of indocyanine green and clinical blood tests including blood urea nitrogen, glucose, bilirubin, albumin, SGPT, and alkaline phosphatase were normal at termination. There was marked right heart dilatation in all dogs. Histologically, the lung demonstrated considerable edema and interstitial thickening in all dogs. The liver showed mild to moderate ischemia and fibrosis. A mathematical model simulating dye clearance in both normal and shunted animals demonstrated increased clearance time in the shunted animal.

LITERATURE CITED

Banaszak, E. F., W. J. Stekiel, R. A. Grace, and J. J. Smith. 1960. Estimation of hepatic blood flow using a single injection dye clearance method. Am. J. Physiol. 198(4):877-880.

Banner, A. S. 1973. Pulmonary function in chronic alcoholism. Am. Rev. Resp. Dis. 108:851-857.

Berthelot, P., J. G. Walker, S. Sherlock, and L. Reid. 1966. Arterial changes in the lungs in cirrhosis of the liver-lung spider nevi. N. Engl. J. Med. 274:291-298.

Bradley, S. E., F. J. Ingelfinger, and G. P. Bradley. 1952. Hepatic circulation in cirrhosis of the liver. Circulation 5:419-429.

Bradley, S. E., C. M. Smythe, H. F. Fitzpatrick, and A. H. Blakemore. 1953. The effect of a portalcaval shunt on estimated hepatic blood flow and oxygen uptake in cirrhosis. J. Clin. Invest. 32:526-537.

Burch, G. E., and N. P. Depasquale. 1967. Alcoholic lung disease - an hypothesis. Am. Heart J. 73(2):147-148.

Byars, T. D., G. V. Lung, N. A. Ferris, and K. S. Keeton. 1976. Activated coagulation time (ACT) of whole blood in normal dogs. Am. J. Vet. Res. 37(11):1359-1361.

Calabresi, P., and W. H. Abelmann. 1957. Porto-caval and porto-pulmonary anastomoses in Laennec's cirrhosis and in heart failure. J. Clin. Invest. 36:1257-1265.

Cameron, G. R. 1948. Pulmonary oedema. Br. Med. J. 1:965-972.

Cotes, J. E., G. B. Field, G. J. A. Brown, and A. E. Read. 1968. Impairment of lung function after portacaval anastomosis. Lancet 1:952-955.

Emirgil, C., and B. J. Sobol. 1977. Pulmonary function in former alcoholics. Chest 72(1):45-51.

Emirgil, C., B. J. Sobol, B. Heymann, and K. Shibutani. 1974. Pulmonary function in alcoholics. Am. J. Med. 57:69-77.

Engwall, M. J. 1980. Changes in pulmonary hemodynamics and lung function associated with an acute intravenous dose of ethanol. M.S. thesis. Iowa State University, Ames.

Heinemann, H. O. 1960. Respiration and circulation in patients with portal cirrhosis of the liver. Circulation 22:154-159.

Heinemann, H. O. 1977. Alcohol and the lung - a brief review. Am. J. Med. 63:81-85.

Johnson, G., and J. Lambert. 1967. Cardiac output after porto-caval shunt. Ann. Surg. 166:207-212.

Lebrec, D., J. P. Capron, D. Dhumeaux, and J. P. Benhamou. 1979. Pulmonary hypertention complicating portal hypertention. Am. Rev. Resp. Dis. 120:849-856.

Lieber, C. S. 1976. The metabolism of alcohol. Sci. Am. 234:25-33.

Markowitz, J., J. Archibald, and H. G. Downie. 1964. Experimental surgery. 5th ed. The Williams and Wilkins Company, Baltimore, Md. 659 pp.

Nakamura, T., S. Nakamura, T. Tazawa, S. Abe, T. Aikawa, and K. Tokita. 1965. Measurement of blood flow through porto-pulmonary anastomosis in portal hypertension. J. Lab. Clin. Med. 65:114-121.

Ruff, F., J. M. B. Hughes, N. Stanley, D. McCarthy, R. Green, A. Aronoff, L. Claton, and J. Milic-Emili. 1971. Regional lung function in patients with hepatic cirrhosis. J. Clin. Invest. 50:2403-2413.

Sallam, M., and W. C. Watson. 1970. Pulmonary hypertension due to micro-thromboembolism from splenic and portal veins after portacaval anastomosis. Br. Heart J. 32:269-271.

Senior, R. M., R. C. Britton, G. M. Turino, J. A. Wood, G. A. Langer, and A. P. Fishman. 1968. Pulmonary hypertension associated with cirrhosis of the liver and with portacaval shunts. Circulation 37:88-96.

Shackelford, R. T. 1955. Bickham-Callendar surgery of the alimentary tract. Vol. 1. W. B. Sanders Co., Philadelphia. 862 pp.

Shaldon, S., J. Caesar, L. Chiandussi, H. S. Williams, E. Sheville, and S. Sherlock. 1961. The demonstration of porta-pulmonary anastomoses in portal cirrhosis with the use of radioactive krypton. N. Engl. J. Med. 265:410-414.

Stekiel, W. J., J. P. Kampine, E. F. Banaszak, and J. J. Smith. 1960. Hepatic clearance of indocyanine in the dog. Am. J. Physiol. 198(4): 881-885.

Swenson, M. J., ed. 1977. Dukes' physiology of domestic animals. 9th ed. Cornell University Press, Ithaca, NY. 914 pp.

Taylor, W. J., and J. D. Myers. 1956. Occlusive hepatic venous catheterization in the study of the normal liver, cirrhosis of the liver and noncirrhotic portal hypertension. Circulation 13:368-380.

West, J. B. 1977. Pulmonary pathophysiology - the essentials. The Williams and Wilkins Company, Baltimore, Md. 227 pp.

Wheeler, H.O., W. I. Cranston, and J. I. Meltzer. 1958. Hepatic uptake and biliary excretion of indocyanine green in the dog. Proc. Soc. Exptl. Biol. Med. 99:11-14.

White, A., P. Handler, and E. L. Smith. 1973. Principles of biochemistry. 5th ed. McGraw-Hill Inc., New York.

Williams, J. H., and W. H. Abelmann. 1963. Portopulmonary shunts in patients with portal hypertension. J. Lab. Clin. Med. 62(5):715-723.

ACKNOWLEDGMENTS

I would like to express my most sincere gratitude to my committee members Dr. Richard Engen, Dr. Richard Seagrave, and Dr. Bernard White for tolerating my lack of knowledge during the course of this research. I would also like to extend my heart-felt thanks to Mrs. Joyce Feavel for her expertise in surgical procedure, Dr. Robert Glock and Dr. John Andrews for their assistance with the pathological aspects of this research, to Mr. Denis Meerdink for the time he spent playing with the computer on my behalf, and to Charm Nickey and Barb Steele for their expert skills used in the preparation of this thesis. Finally, I wish to extend my thanks and gratitude to Mr. Mark Darrah for helping me find the courage and the intestinal fortitude to keep going when I wanted to quit.

APPENDIX A: SURGICAL PROCEDURE

The following is a detailed description of the methods used to create a porto-caval shunt from the procedure for performing an Eck fistula, as described by Markowitz et al. (1964, pp. 542-546).

After fasting 24 hours, each dog was anesthetized with sodium pentobarbital (28.6 mg/kg). The animal was then intubated and prepared for surgery by shaving hair from dorsal to ventral midline on the right side extending from mid-thorax to the hind limb. Following preparation of the surgical site asceptically, the animal was placed on the table in dorsal recumbency with exposure favoring the lateral right side. The table was equipped with a circulating heating water pad to control body temperature during the procedure.

The incision was made starting from the xiphoid process down the midline for approximately 4 cm, then down at an angle paralleling the costal margin to just beyond the nipple line, extending to about the level of the umbilicus. Stay sutures were placed on the muscle groups to be incised to aid in alignment on closure and care was taken to control bleeding as the Rectus abdominus, internal abdominal oblique, a section of the external abdominal oblique, and the Transversus abdominus were cut. Upon entering the peritoneum, the incision was retracted and after wrapping the viscera in the mesenteric membrane, the viscera were removed from the cavity and placed in a moist, sterile turkish towel and placed to the left side of the animal.

After stripping fat and overlying fascia away from both portal vein and vena cava, stay sutures were placed (Figure 7) using 5-0 cardio-

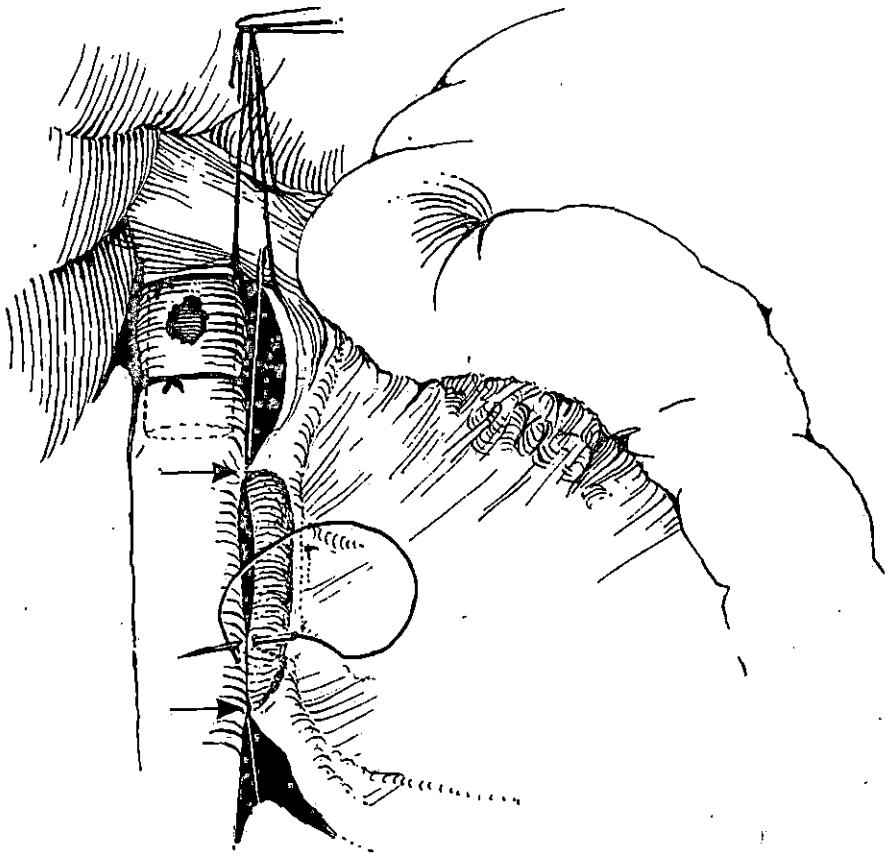

Figure 7. The Eck fistula; the portal vein (right) has been attached to the vena cava (left) by stay sutures (arrows) and the posterior suture line is laid with the bottom needle. (Markowitz et al., 1964, p. 550, figure XXVIII-25)

vascular silk to attach the two vessels together. Two needles were used for the two stay sutures and the needles were left intact for the next step.

A posterior suture line was then placed continuously between the two vessels using a length of 5-0 silk distal to the liver. Care was taken to control bleeding as the needle was passed through the portal wall, as the wall is very thin and tears quite easily.

Upon completion of the posterior suture line, a cutting thread of 1-0 gastrointestinal silk was then placed in both vessels near and parallel to the suture line (Figure 8a).

After the cutting thread was placed, the 5-0 silk proximal to the liver was used to place the anterior suture line in the same manner as before (Figure 8B). When completed, the two vessels are aligned (Figure 8C) with the cutting thread buried between them.

The cutting thread was carefully pulled free in a back-and-forth motion, cutting the walls of both vessels and creating the fistula in the process. In some cases, there was some bleeding from the exit point of the cutting thread which was controlled by placing a single interrupted suture of 5-0 silk to further close the exit point.

Once it was certain hemostasis had been achieved, the viscera were replaced, the retractor removed, and the incision was closed using 3-0 silk in a continuous pattern, taking care to align the layers of muscle and fascia. The skin was closed using Vetafil^{R} (S. Jackson, Inc., Washington, DC) in a single interrupted pattern.

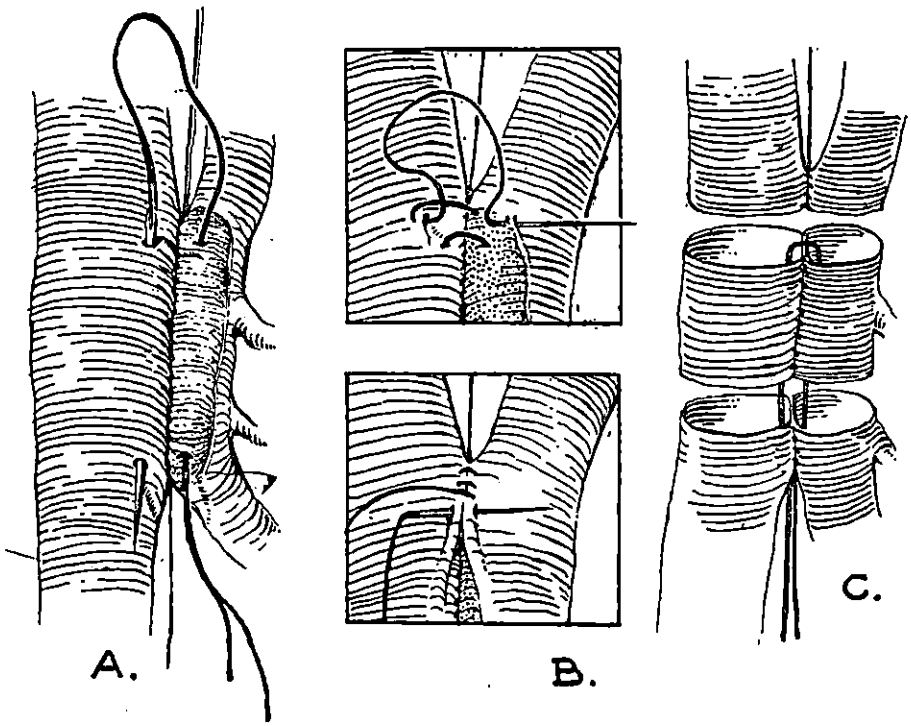

Figure 8. The Eck fistula; the portal vein is on the right and the vena cava is on the left. A) The cutting thread is introduced parallel to the posterior suture line. This thread will create the fistula when pulled free. B) The anterior suture line draws both vessels together and buries the cutting thread between the two vessels. C) Principle of action of the cutting thread. The vessels are aligned as shown in cross-section. Pulling the cutting thread free will complete the fistula. (Markowitz et al., 1964, p. 551, figure XXVIII-26)

The technique described above was slightly modified from the original description (Markowitz et al., 1964) in that the portal vein was not ligated following completion of the fistula. The author felt this would simulate the actual conditions of advanced liver disease more closely than a complete shunt.

APPENDIX B: CALCULATION PROGRAMS FOR TI-55 CALCULATOR

Compliance-Resistance Program

Key stroke	Step	Key code	Key stroke	Step	Key code
RCL	00	61	=	16	85
2	01	02	÷	17	45
÷	02	45	RCL	18	61
RCL	03	61	0	19	00
4	04	04	=	20	85
=	05	85	R/S	21	86
R/S	06	86	RST	22	87
1/X	07	34	-	23	00
X	08	55	-	24	00
RCL	09	61	-	25	00
1	10	01	-	26	00
=	11	85	-	27	00
+/-	12	84	-	28	00
+	13	75	-	29	00
RCL	14	61	-	30	00
3	15	03	-	31	00

Memory locations	Value for
STO 0	Flow (F)
STO 1	Tidal volume at a flow (V_{TF})
STO 2	Tidal volume (V_T)
STO 3	Pressure at a flow (P_{TF})
STO 4	Esophageal pressure (P_T)

Procedure

1) Store values from Dynagraph recordings into memory.

2) Push run (R/S) key - display shows calculated compliance (C_L).

3) Push run key again - display shows calculated resistance (R).

Functional Residual Capacity Program

Key stroke	Step	Key code	Key stroke	Step	Key code
STO	00	51	R/S	16	86
0	01	00	STO	17	51
X⇄Y	02	31	1	18	01
SUM	03	71	X⇄Y	19	31
0	04	00	+/-	20	84
R/S	05	86	SUM	21	71
STO	06	51	1	22	01
1	07	01	EXC	23	66
X⇄Y	08	31	1	24	01
+/-	09	84	1/X	25	34
SUM	10	71	PROD	26	76
1	11	01	0	27	00
EXC	12	66	RCL	28	61
1	13	01	0	29	00
PROD	14	76	R/S	30	86
0	15	00	RST	31	87

Memory locations 0 and 1 are used for temporary purposes.

Procedure

1) Enter deadspace volume (V_{DS}) = 45.0.

2) Push interchange key (X⇄Y).

3) Enter expired air volume (V_E).

4) Push run (R/S) key - disregard display.

5) Enter nitrogen content of inspired oxygen (F_I).

6) Push interchange key.

7) Enter nitrogen content of expired air (F_E).

8) Push run key - disregard display.

9) Enter post-washout alveolar nitrogen content (F_A).

10) Push interchange key.

11) Enter pre-washout alveolar nitrogen content (F_0).

12) Push run key - display shows calculated FRC.

Percentage Disappearance Rate Program

Key stroke	Step	Key code	Key stroke	Step	Key code
STO	00	51	RCL	16	61
1	01	01	3	17	03
X⇄Y	02	31	=	18	85
÷	03	45	INV	19	21
RCL	04	61	PROD	20	76
1	05	01	2	21	02
=	06	85	RCL	22	61
lnX	07	23	2	23	02
STO	08	51	e^x	24	24
2	09	02	+/-	25	84
R/S	10	86	+	26	75
STO	11	51	1	27	01
3	12	03	=	28	85
X⇄Y	13	31	R/S	29	86
+/-	14	84	RST	30	87
+	15	75	-	31	00

Memory locations 1, 2, and 3 are temporary only.

Procedure

1) Enter value for C_2.

2) Push interchange key (X⇄Y).

3) Enter value for C_1.

4) Push run (R/S) key.

5) Enter value for T_1.

6) Push interchange key (X⇄Y).

7) Enter value for T_2.

8) Push run (R/S) key.

9) Multiply display value by 100.

10) Display shows calculated percentage disappearance rate.

APPENDIX C: CLINICAL TEST RESULTS

Test	Dog # 1588	1598	1656	1704	1740
Urea nitrogen (mg/dl)	12	18	18	21	16
Glucose (mg/dl)	102	75	93	81	89
Total bilirubin (mg/dl)	<1.0	<1.0	<1.0	<1.0	<1.0
Direct bilirubin (mg/dl)	<1.0	<1.0	<1.0	<1.0	<1.0
Albumin (gm/dl)	3.6	3.3	4.1	3.2	3.0
SGPT (IU/l)	19.2	15.4	17.5	15.7	62.4
Alkaline phosphatase (IU/l)	39.7	24.9	28.0	29.0	26.3
Activated clotted time (sec)	102	115	129	97	96

APPENDIX D: POST-MORTEM OBSERVATIONS

The following observations were made at termination for the six dogs used in this project. Included are gross as well as histopathological observations, as determined by Dr. Robert Glock, Department of Veterinary Pathotogy, Iowa State University, and Dr. John Andrews, Diagnostic Laboratory, College of Veterinary Medicine, Iowa State University.

Gross Observations

Observations were made only if organ or tissue had visible signs of abnormality. All other normal tissues were not listed. The animal's breed, sex, weight, and time since surgery are given.

Dog #1582: Irish Setter, male, 22.7 kg, 43 weeks. The lung had raised grey plaques 1-2 cm on both diaphragmatic lobes and what appeared to be pleural thickening. There was moderate right heart dilatation.

Dog #1588: Husky, female, 25.4 kg, 33 weeks. Hair on right side never grew back after surgery and numerous skin lesions were noted. The brain had moderate internal hydrocephalus. The liver was 740 gm and appeared slightly congested with rounded edges. The heart showed very mild right heart dilatation with a calcified plaque on the endocardial surface of the right ventricular wall. The kidneys were normal except for a surgical sponge adhered to the anterior pole of the right kidney. There was a mass of adhesions in the mesentery.

Dog #1598: Terrier-Hound, female, 16.3 kg, 34 weeks. The left lung was mildly congested. The heart showed mild right heart dilatation. The

liver was 640 gm and appeared normal. The jejunum showed a moderately roughened mucosa due to heavy hookworm infestation.

Dog #1656: Labrador-Irish Setter, male, 13.2 kg, 33 weeks. The heart showed considerable right heart dilatation. The liver was 550 gm and was mildly congested. There was still evidence of subcutaneous infection at the suture line with numerous fistulous tracts under the skin.

Dog #1704: Collie-Mixed, female, 15.9 kg, 29 weeks. The heart showed moderate right heart dilatation. The liver was 830 gm and showed moderate congestion. There was a mild hookworm infestation.

Dog #1740: Golden Retriever, male, 17.7 kg, 32 weeks. The heart showed very mild right heart dilatation. The liver was 1000 gm and was moderately congested. There was thickening of the jejunal mucosa and blood spots were evident due to a moderate hookworm infestation.

Histopathological Observations

Dog #1582 (Case #8J-R-1142): Time since surgery = 43 weeks.

Slide	Tissue	Description
A	Kidney	NML (no major lesions)
F	Kidney	NML
B,E	Liver	Centrilobular veins fibrotic and mildly infiltrated with mononuclear cells. Hepatic cords disorganized and centrilobular hepatocytes vacuolated. Diffuse retention of bile in the hepatocytes noted.
C	Lung	Moderate interstitial thickening throughout the section. Lesion in one end showed consolidation with macrophages and some interstitial fibrosis. A few alveoli contained neutrophils.

G	Lung	Moderate interstitial thickening and considerable smooth muscle hypertrophy around terminal bronchioles. Mild anthracosis noted.
D	Spleen	Moderate lymphoid depletion.
F	Thyroid	NML
F	Parathyroid	NML
G	Heart	NML
H	Adrenal	NML

Dog #1588 (Case #80-R-1141): Time since surgery = 33 weeks.

A-D	Brain	NML
E	Kidney	NML
F	Lung	Moderate congestion and interstitial thickening.
I	Lung	Moderately congested.
K	Lung	NML
G	Liver	Congested with fibrosis around centrilobular veins.
I	Liver	Congested with fibrosis.
G	Spleen	Congested.
H	Thyroid	NML
H	Parathyroid	NML
H	Jejunum	NML
J	Heart	Adipose cells scattered throughout. An area of bone and cartilage on endocardial surface.
L	Jejunum	NML
M	Skin	Marked hyperkeratosis and very thin epithelium.

Dog #1598 (Case #80-R-1143): Time since surgery = 34 weeks.

A-D	Brain	NML

E	Kidney	Several very small foci of mononuclear inflammatory cells.
F,J,M	Liver	Mild diffuse fatty change. Severe fibrosis and mononuclear infiltration of central veins. Some recanalization present.
G	Lung	Areas of mild to marked interstitial fibrosis. Alveoli contain leukocytes, some of which were heart failure cells.
I	Lung	Mild to moderate interstitial thickening and some smooth muscle hypertrophy.
H	Jejunum	NML except for one embedded hookworm.
I	Thyroid	NML
K	Jejunum	NML
L	Heart	NML
H	Lung	NML
H	Thyroid	NML
H	Parathyroid	NML
I	Jejunum	NML
K	Spleen	Very congested.
L	Heart	Adipose cells scattered in myocardium.

Dog #1656 (Case, #80-R-1139): Time since surgery = 33 weeks.

A-C	Brain	NML
D	Kidney	Congested.
E	Liver	Congested around central veins and sinusoids. Central veins surrounded by fibrin and very early fibrosis. Areas of inflammatory cell infiltration around portal and central vessels. Some of these areas contained numerous eosinophils.
G	Liver	Same as slide E plus some mild fatty change.
F,J	Lung	Generalized congestion and focal areas of mild interstitial thickening.

H	Lung	NML
H	Thyroid	NML
H	Parathyroid	NML
I	Jejunum	NML
K	Spleen	Very congested.
L	Heart	Adipose cells scattered in myocardium.

Dog #1704 (Case #80-R-1140): Time since surgery = 29 weeks.

A-C	Brain	NML
D	Kidney	Mildly congested.
E	Liver	Moderately congested.
I	Liver	Moderately congested.
E,F,J	Lung	Mildly congested.
G	Heart	NML
G	Thyroid	NML
G	Parathyroid	NML
H	Jejunum	NML
J	Lymph Node	NML
K	Spleen	Congested.

Dog #1740 (Case #80-R-1144): Time since surgery = 32 weeks

A-C	Brain	NML
D	Kidney	NML
E,F,J	Liver	Marked congestion with edema, fibrin, mononuclear cells, and mild fibrosis around central veins.
G	Lung	Congestion.
H	Spleen	Some dilatation of veins in traveculae.

I	Jejunum	NML
K	Heart	NML
L	Thyroid	NML
L	Lymph Node	NML

APPENDIX E: MATHEMATICAL MODEL FOR CLEARANCE OF INDOCYANINE GREEN

CASE I: no shunt

rate of destruction in liver = -KQC
KQ = "clearance"

Dye in blood

$$(1)\quad V_B \frac{dC}{dt} = (Q_m + Q_H)C_L - Q_H C - Q_m C$$

accum. in blood (neg)	dye returning from liver	dye flowing to liver via hepatic artery	dye flowing to liver from portal vein

Overall

$$(2)\quad Q_L = Q_m + Q_H$$

Dye in liver

$$(3)\quad V_L \frac{dC_L}{dt} = (Q_m + Q_H)C - (Q_m + Q_H)C_L - K(Q_m + Q_H)C_L$$

accum. in liver (neg)	into liver	out of liver	destruction	$K(Q_m + Q_H)$ = liver dye clearance

Solutions: from (1) and (2) - substituting and rearranging

$$(4)\quad V_B \frac{dC}{dt} = Q_L C_L - (Q_H + Q_m)C = Q_L C_L - Q_L C$$

$$(5)\quad \frac{d\overline{C}}{dt} = \frac{Q_L}{V_B}(\overline{C}_L - \overline{C})$$

from (2) and (3) - substitute and rearrange

$$(6)\quad V_L \frac{dC_L}{dt} = Q_L C - Q_L C_L - KQ_L C_L$$

$$(7)\quad \frac{dC_L}{dt} = \frac{Q_L}{V_L}(C - C_L) - \frac{KQ_L}{V_L} C_L$$

mult. in/out term by $\frac{V_B}{V_B}$

$$\frac{d\bar{C}_L}{dt} = \frac{Q_L}{V_B} \cdot \frac{V_B}{V_L} (\bar{C} - \bar{C}_L) - \frac{KQ_L}{V_L} \bar{C}_L \quad \text{where } \bar{C}(0) = 1, \; C_L(0) = 0 \tag{8}$$

CASE II: shunt

σ = fraction of blood shunted to vena cava
$\rho = (1 - \sigma)$ = fraction of portal blood left after shunt
$\sigma > 0$, $\rho < 1$

Same eqns. hold except: $Q_L' = Q_H + \rho Q_m$ where $\frac{Q_L'}{Q_L} = \frac{Q_H + \rho Q_m}{Q_H + Q_m}$

Solutions:

$$(9) \quad \frac{d\bar{C}'}{dt} = \frac{Q_L'}{V_B} (\bar{C}_L' - \bar{C}')$$

$$(10) \quad \frac{d\bar{C}_L'}{dt} = \frac{Q_L'}{V_B} \cdot \frac{V_B}{V_L} (\bar{C}' - C_L') - \frac{KQ_L'}{V_L} \bar{C}_L' \quad \text{where } \bar{C}'(0) = 1, \; \bar{C}_L'(0) = 0$$

When Q_L' is reduced, $\tau'(\frac{V_B}{Q_L'})$ is lengthened, clearance is reduced.

General solution:

I - no shunt: let $\frac{Q_L}{V_B} = 1/\tau$, $v = \frac{V_B}{V_L}$, $K = \frac{KQ_L}{V_L}$, take derivative of 5

from (5) $$\frac{d^2\bar{C}}{dt^2} = \frac{1}{\tau} (\frac{d\bar{C}_L}{dt} - \frac{d\bar{C}}{dt}) \tag{11}$$

Subst. (8) for $\frac{dC_L}{dt}$ into (11)
$$\frac{d^2\bar{C}}{dt^2} = \frac{1}{\tau} [[\frac{v}{\tau}(\bar{C} - \bar{C}_L) - K\bar{C}_L] - \frac{d\bar{C}}{dt}] \tag{12}$$

Solving (5) for C_L
$$\bar{C}_L = \tau \frac{d\bar{C}}{dt} + \bar{C} \tag{13}$$

Subst. (13) into (12) for C_L

$$\frac{d^2\bar{C}}{dt^2} = \frac{1}{\tau}\left[\left[\frac{v}{\tau}\left(\bar{C} - \left(\tau\frac{d\bar{C}}{dt} + \bar{C}\right)\right) - K\left(\tau\frac{d\bar{C}}{dt} + \bar{C}\right)\right] - \frac{d\bar{C}}{dt}\right] \quad (14)$$

drop ( ) and condense

$$\frac{d^2\bar{C}}{dt^2} = \frac{1}{\tau}\left[\left[\frac{v}{\tau}\left(\bar{C} - \tau\frac{d\bar{C}}{dt} - \bar{C}\right) - K\tau\frac{d\bar{C}}{dt} - \frac{K\bar{C}}{\tau}\right] - \frac{1}{\tau}\frac{d\bar{C}}{dt}\right] \quad (15)$$

$$\frac{d^2\bar{C}}{dt^2} = -\frac{v}{\tau}\frac{d\bar{C}}{dt} - K\frac{d\bar{C}}{dt} - \frac{K\bar{C}}{\tau} - \frac{1}{\tau}\frac{d\bar{C}}{dt} \quad (16)$$

$$\frac{d^2\bar{C}}{dt^2} = -\left[\left(\frac{v}{\tau} + K + \frac{1}{\tau}\right)\frac{d\bar{C}}{dt}\right] - \frac{K\bar{C}}{\tau} \quad (17)$$

rearranging to final form

$$\frac{d^2\bar{C}}{dt^2} + \left(K + \frac{1}{\tau} + \frac{v}{\tau}\right)\frac{d\bar{C}}{dt} + \left(\frac{K}{\tau}\right)\bar{C} = 0 \quad (18)$$

where $\bar{C}(0) = 1$, $\frac{d\bar{C}}{dt}(0) = 1/\tau$ from (5)

general form

$$A\frac{d^2\bar{C}}{dt^2} + B\frac{d\bar{C}}{dt} + C'\bar{C} = 0 \quad (19)$$

general solution

$$C(t) = De^{-mt} \quad (20)$$

first derivative

$$\frac{dC}{dt} = -mDe^{-mt} \quad (21)$$

second derivative

$$\frac{d^2C}{dt^2} = +m^2De^{-mt} \quad (22)$$

substituting (20-22) into (19)

$$Am^2De^{-mt} - BmD^{-mt} + C'De^{-mt} = 0 \quad (23)$$

factoring De^{-mt} and mult. by $1/De^{-mt}$

$$Am^2 - Bm + C = 0 \quad (24)$$

solving for m using quadratic eqn.

$$m_1 = \frac{B + \sqrt{B^2 - 4AC}}{2A}, \quad m_2 = \frac{B - \sqrt{B^2 - 4AC}}{2A} \quad (25)$$

general solution

$$C(t) = D_1e^{-m_1t} + D_2e^{-m_2t} \quad (26)$$

from (18) $C(0) = D_1 + D_2 = 1$ (27)

from (26) and (18) $\frac{dC}{dt}(0) = -m_1D_1e^{-mt} - m_2D_2e^{-m2t} = -1/\tau$ (28)

simplifying $m_1D_1 + m_2D_2 = 1/\tau$ (29)

from (27) $D_2 = 1 - D_1$ (30)

substituting into (29) $m_1D_1 + m_2(1 - D_1) = 1/\tau$ (31)

from (25) $(\frac{B + \sqrt{B^2 - 4AC}}{2A})D_1 + (\frac{B - \sqrt{B^2 - 4AC}}{2A})$

$- (\frac{B - \sqrt{B^2 - 4AC}}{2A})D_1 = 1/\tau$ (32)

from (18) and (19) $A = 1$ (33)

from (32), multiply by 2 $(B + \sqrt{B^2 - 4C})D_1 + (B - \sqrt{B^2 - 4C})$

$- (B - \sqrt{B^2 - 4C})D_1 = 2/\tau$ (34)

combining similar terms and simplifying $(B + \sqrt{B^2 - 4C} - B + \sqrt{B^2 - 4C})D_1$

$+ (B - \sqrt{B^2 - 4C}) = 2/\tau$ (35)

$(2\sqrt{B^2 - 4C})D_1 + B - \sqrt{B^2 - 4C} = 2/\tau$ (36)

solving for D_1 $D_1 = \frac{2/\tau - B + \sqrt{B^2 - 4C}}{2\sqrt{B^2 - 4C}}$ (37)

simplifying $D_1 = 1/\tau(B^2 - 4C)^{-1/2} - \frac{B}{2}(B^2 - 4C)^{-1/2} + 1/2$ (38)

solving for D_2 from (30) $D_2 = -1/\tau(B^2 - 4C)^{-1/2} + \frac{B}{2}(B^2 - 4C)^{-1/2} + 1/2$ (39)

from (18) and (19) $B = (K + 1/\tau + v/\tau)$ (40)

$C = (K/\tau)$ (41)

substituting (40-41), (38-39), and (25) into (26)

$$C(t) = \{\tfrac{1}{\tau}[(K + 1/\tau + v/\tau)^2 - \tfrac{4K}{\tau}]^{-1/2} - [\tfrac{1}{2}(K + 1/\tau + v/\tau)][(K + 1/\tau + v/\tau)^2 - \tfrac{4K}{\tau}]^{-1/2} + 1/2\}_e - [\frac{(K + 1/\tau + v/\tau) + \sqrt{(K + 1/\tau + v/\tau)^2 - \frac{4K}{\tau}}}{2}]t + \{-\tfrac{1}{\tau}[(K + 1/\tau + v/\tau)^2 - \tfrac{4K}{\tau}]^{-1/2} + [\tfrac{1}{2}(K + 1/\tau + v/\tau)][(K + 1/\tau + v/\tau)^2 - \tfrac{4K}{\tau}]^{-1/2} + 3/2\}_e - [\frac{(K + 1/\tau + v/\tau) - \sqrt{(K + 1/\tau + v/\tau)^2 - \frac{4K}{\tau}}}{2}]t \quad (42)$$

factoring and simplifying

$$C(t) = \{[\tfrac{1}{\tau} - \tfrac{1}{2}(K + 1/\tau + v/\tau)][(K + 1/\tau + v/\tau)^2 - \tfrac{4K}{\tau}]^{-1/2} + 1/2\}_e - [\frac{(K + 1/\tau + v/\tau) + \sqrt{(K + 1/\tau + v/\tau)^2 - \frac{4K}{\tau}}}{2}]t + \{[-1/\tau + \tfrac{1}{2}(K + 1/\tau + v/\tau)][(K + 1/\tau + v/\tau)^2 - \tfrac{4K}{\tau}]^{-1/2} + 1/2\}_e - [\frac{(K + 1/\tau + v/\tau) - \sqrt{(K + 1/\tau + v/\tau)^2 - \frac{4K}{\tau}}}{2}]t \quad (43)$$

final form - normal

$$C(t) = \{[(v+1)/2\tau + 1/\tau - K/2][(K + 1/\tau + v/\tau)^2 - \tfrac{4K}{\tau}]^{-1/2} + 1/2\}_e - [\frac{(K + 1/\tau + v/\tau) + \sqrt{(K + 1/\tau + v/\tau)^2 - \frac{4K}{\tau}}}{2}]t + \{[(v+1)/2\tau - 1/\tau + K/2][(K + 1/\tau + v/\tau)^2 - \tfrac{4K}{\tau}]^{-1/2} + 1/2\}_e - [\frac{(K + 1/\tau + v/\tau) - \sqrt{(K + 1/\tau + v/\tau)^2 - \frac{4K}{\tau}}}{2}]t \quad (44)$$

II - with shunt: let $\frac{Q_L'}{V_B} = 1/\tau'$, $V = V_B/V_L$, $K' = \frac{KQ_L'}{V_L}$

final form - shunt Q.E.D.

$$C(t) = \{[(v+1)/2\tau' + 1/\tau' - K'/2][K' + 1/\tau' + v/\tau')^2 - \frac{4K'}{\tau'}]^{-1/2} + 1/2\}_e$$

$$- [\frac{(K + 1/\tau' + v/\tau') + \sqrt{(K' + 1/\tau' + v/\tau')^2 - \frac{4K'}{\tau'}}}{2}]t + \{[v/\tau + K'] \cdot$$

$$+ \{[(v+1)/2\tau' - 1/\tau' + K'/2][(K' + 1/\tau' + v/\tau')^2 - \frac{4K'}{\tau'}]^{-1/2} + 1/2\}_e$$

$$- [\frac{(K' + 1/\tau' + v/\tau') - \sqrt{(K' + 1/\tau' + v/\tau')^2 - \frac{4K'}{\tau'}}}{2}]t \qquad (45)$$

Variable assignments:

Normal:

Independent	Dependent
QM - portal flow	QL = QH + QM
QH - hepatic arterial flow	TA = VB/QL
VB - blood volume, total	V = VB/VL
VL - blood volume, liver	KU = KL*QL/VL
KL - dye clearance constant	
	A1 = (KU + 1/TA + V/TA)
	A2 = FSQT(A1↑2-4*KU/TA)
	B1 = (v+1)/2*TA + 1/TA - KU/2
	B2 = (v+1)/2*TA - 1/TA + KU/2

Shunt:

Independent	Dependent
QM	QK = QH + R*QM
QH	TB = VB/QK
VB same as normal	KV = KL*QK/VL
VL " "	A3 = (KV + 1/TB + V/TB)
KL	A4 = FSQT(A3↑2-4*KV/TB)
R - blood fraction to liver	B3 = (v+1)/2*TB + 1/TB - KV/2
	B4 = (v+1)/2*TB - 1/TB + KV/2

Program:

```
1.1  F I=Ø, 24Ø; S Z=FDIS(I,Ø); S Z=FDIS(Ø,I)
1.2  F I=Ø, 1Ø, 230; DO 2

2.1  F J=Ø,5; S Z=FDIS(I,J); S Z=FDIS(J,I)

3.1  ASK QM,QH,VB,VL,KL,R
3.2  S QL = QH+QM; S TA=VB/QL; S V=VB/VL; S KU=KL*QL/VL
3.3  S A1 = KU + 1/TA+V/TA; S A2=FSQT(A1↑2-4*KU/TA)
3.4  S B1 = (v+1)/2*TA + 1/TA - KU/2; S B2 = (v+1)/2*TA - 1/TA + KU/2
3.5  S QK=QH+R*QM; S TB=VB/QK; S KV=KL*QK/VL
```

```
3.6  S A3=KV+1/TB+V/TB; S A4=FSQT(A3↑2-4*KV/TB)
3.7  S B3=(v+1)/2*TB+1/TB-KV/2; S B4=(v+1)/2*TB-1/TB+KV/2

4.1  F T=1, 200; DO 5

5.1 S CN=(B1/A2+0.5)*FEXP(((-A1-A2)/2)*T)+(B2/A2+0.5)*FEXP(((-A1+A2)/2)*T)
5.2 S CS=(B3/A4+0.5)*FEXP(((-A3-A4)/2)*T)+(B4/A4+0.5)*FEXP(((-A3+A4)/2)*T)
5.3 S Z=FDIS(T,50+CN*50); S Z=FDIS(T,50+CS*50)
```

Parameters: (Swenson, 1977)

BW = 22.7 kg
C.0 = 165 ml/kg/min = 3746 ml/min
*VB = 92 ml/kg = 2090 ml
*VL = 0.07 VB = 146 ml
QL = 40 ml/kg/min = 908 ml
*QH = 1/3 QL = 303 ml
*QM = 2/3 QL = 605 ml
*KL < 0.5 mg/min
*0 < R < 1 (*computer variables)

Half-time calculation:

from (26) take log both sides

$$\log C = \log(D_1 e^{-m_1 t}) + \log (D_2 e^{-m_2 t} \tag{46}$$

$$\log C = \log(D_1) + \log e^{-m_1 t} + \log D_2 + \log e^{-m_2 t} \tag{47}$$

grouping log terms on left side and factoring right side

$$\log C - \log D_1 - \log D_2 = (-m_1 - m_2)t \tag{48}$$

solving for t

$$t = \frac{\log C - \log D_1 - \log D_2}{(-m_1 - m_2)} \tag{49}$$

for normal case

$$T_{\frac{1}{2}} = \frac{\log C - \log D_1 - \log D_2}{(-m_1 - m_2)} \tag{50}$$

for shunt case

$$T_{\frac{1}{2}}' = \frac{\log C - \log D_1' - \log D_2'}{(-m_1' - m_2')} \tag{51}$$

For $t_{1/2}$, let C = 0.5.

Program:

```
6.1 S D1=B1/A2+0.5; S D2=B2/A2+0.5; S M1=(-A1-A2)/2; S M2=(-A1+A2)/2
6.2 S D3=B3/A4+0.5; S D4=B4/A4+0.5; S M3=(-A3-A4)/2; S M4=(-A3+A4)/2
6.3 S T1=(FLOG(0.5)-FLOG(D1)-FLOG(D2))/(-M1-M2)
6.4 S T2=(FLOG(0.5)-FLOG(D3)-FLOG(D4))/(-M3-M4)
6.5 S T3=(T1/T2)*100
6.6 T T1,T2,T3!
```